Localised axial progenitor cell populations in the avian tail bud are not committed to a posterior Hox identity

Michael J. McGrew[1], Adrian Sherman[1], Simon G. Lillico[1], Fiona M. Ellard[2], Pippa A. Radcliffe[2], Hazel J. Gilhooley[1], Kyriacos A. Mitrophanous[2], Noemí Cambray[3], Valerie Wilson[3],* and Helen Sang[1,*,†]

The outgrowth of the vertebrate tail is thought to involve the proliferation of regionalised stem/progenitor cell populations formed during gastrulation. To follow these populations over extended periods, we used cells from GFP-positive transgenic chick embryos as a source for donor tissue in grafting experiments. We determined that resident progenitor cell populations are localised in the chicken tail bud. One population, which is located in the chordoneural hinge (CNH), contributes descendants to the paraxial mesoderm, notochord and neural tube, and is serially transplantable between embryos. A second population of mesodermal progenitor cells is located in a separate dorsoposterior region of the tail bud, and a corresponding population is present in the mouse tail bud. Using heterotopic transplantations, we show that the fate of CNH cells depends on their environment within the tail bud. Furthermore, we show that the anteroposterior identity of tail bud progenitor cells can be reset by heterochronic transplantation to the node region of gastrula-stage chicken embryos.

KEY WORDS: Progenitor cell, Tail bud, Chordoneural hinge, Hox genes, Transgenic chicken

INTRODUCTION

During gastrulation, the three germ layers of the embryo are formed by cell ingression from the epiblast through the primitive streak. These cells take up residence along the developing anteroposterior axis of the body during primitive streak elongation and regression. In the chick, as in other vertebrates, closure of the posterior neuropore ends the process known as primary body development, driven by the primitive streak. Further (secondary body) development derives from a caudal cap of tissue, the tail bud, which generates the region from the lumbosacral vertebrae to the tip of the tail (Homdahl, 1925; Gaertner, 1949; Seichart and Jelinek, 1968) (reviewed by Stern et al., 2006). The primitive streak and tail bud thus supply cells to the neural tube and mesoderm over the entire post-cranial axis (Schoenwolf, 1977; Schoenwolf, 1979a; Catala et al., 1995; Psychoyos and Stern, 1996). Tail bud outgrowth differs morphologically from earlier gastrula stages in several respects. Formation of the neural tube in the tail bud results from cavitation of the medullary cord, and is distinct from primary neurulation, which occurs by the folding and fusion of the dorsal edges of the neural plate (Criley, 1969; Kilka and Jelinek, 1969; Schoenwolf and Delongo, 1980). The nascent embryonic chick tail subsequently undergoes reduction and remodeling by selective proliferation, involution and cell death (Lanot, 1980; Schoenwolf, 1981; Sanders et al., 1986; Uehara and Ueshima, 1988; Miller and Briglin, 1996).

Despite these differences, similarities in gene expression patterns in the primitive streak and tail bud (Gont et al., 1993; Gofflot et al., 1997; Knezevic et al., 1998; Cambray and Wilson, 2007), and the analysis of morphogenic movements in the streak and tail bud (Pasteels, 1937; Gont et al., 1993; Catala et al., 1995; Kanki and Ho, 1997; Knezevic et al., 1998), reveal many commonalities between these two processes in several vertebrate species. Additionally, mutation studies show that several genes, including members of the Wnt gene family and brachyury, have a role during both primitive streak and tail bud outgrowth in mouse (Herrmann et al., 1990; Greco et al., 1996; Yamaguchi et al., 1999) and zebrafish (Marlow et al., 2004). This evidence supports the view, as first proposed by Pasteels (Pasteels, 1943), that many aspects of tail bud outgrowth are continuations of the gastrulation process.

Further morphological, gene expression and cell lineage studies have shown that distinct sub-domains of the primitive streak are analogous to those in the tail bud in chicken (Catala et al., 1995; Knezevic et al., 1998), mouse (Cambray and Wilson, 2002; Cambray and Wilson, 2007) and *Xenopus* (Gont et al., 1993; Tucker and Slack, 1995; Davis and Kirschner, 2000). The node region (equivalent to the organizer in *Xenopus* and zebrafish) contains progenitor cells of the neural tube, notochord and somites. It also gives rise to cells that contribute to the chordoneural hinge (CNH) in the tail bud, a region where the posterior end of the notochord abuts the overlying neural tube (Pasteels, 1943). Like the earlier node, the CNH contributes progeny to the neural tube, notochord and paraxial mesoderm (Catala et al., 1995; Davis and Kirschner, 2000; Cambray and Wilson, 2002). The continuous generation of neural tube, notochord and somites by the node region and CNH, which apparently contain resident cells, is consistent with the hypothesis that these regions contain multipotent stem cells, i.e. cells that are capable of giving rise to both further axial progenitor cells in the streak/tail bud and differentiated cells of multiple lineages in the axis.

A number of reports lend support to this idea. Specifically, single-cell labeling experiments in the chick and mouse node during gastrulation suggest that some cells are resident there, contributing descendants over significant axial stretches to notochord, neural tube and somites (Selleck and Stern, 1991; Selleck and Stern, 1992; Lawson et al., 1991). Retrospective clonal analysis in the mouse also indicates that the progenitors of the myotome (a somite derivative) and spinal cord undergo stem cell divisions (Nicolas et al., 1996; Mathis and Nicolas, 2000; Eloy-Trinquet and Nicolas, 2002; Roszko

[1]The Roslin Institute and Royal Dick School of Veterinary Studies, University of Edinburgh, Roslin, Midlothian, UK. [2]Oxford Biomedica (UK) Ltd, Medawar Centre, Oxford Science Park, Oxford, UK. [3]Institute for Stem Cell Research, MRC Centre for Regenerative Medicine, University of Edinburgh, Edinburgh, UK.

*Joint senior authors
†Author for correspondence (e-mail: helen.sang@bbsrc.ac.uk)

et al., 2007). Technical issues have so far prevented prospective single-cell lineage analyses on the node's descendant in the tail bud, the CNH. However, grafting experiments suggest that this region may contain the stem cell progenitors of these tissues, as inferred from the retrospective studies mentioned above. Serial grafts of the CNH to early somite-stage embryos result in continued retention of graft-derived cells in the CNH, as well as exit of cells and contribution along the body axis (Cambray and Wilson, 2002).

Despite the evidence that individual cells reside in the streak and contribute over long axial distances, these cells, elsewhere termed 'stem cells', do not strictly self-renew (i.e. give rise to exact copies of themselves) in vivo, as their gene expression changes over time (Iimura and Pourquié, 2006; Cambray and Wilson, 2007). For this reason, and because the processes of primary and secondary body development are different, we refer to resident cells as long-term axial progenitors (LTAPs), and to a population of cells that behaves in this way as a LTAP population. Short-term axial progenitors (STAPs) are cells in the streak/tail bud that exit these regions and populate limited axial regions. It should be noted that the term 'LTAP population' is conceptually equivalent to the neural 'stem zone', defined in chick, where labeled groups of cells give rise to descendants in both the neural tube and the tail bud; the population as a whole thus behaves as if it contains resident cells (Brown and Storey, 2000).

When mouse tail bud CNH progenitor cells, which would normally populate posterior tail somites, were grafted to the node/primitive streak region in earlier embryos, they populated more anterior axial levels, suggesting that they were not committed to a particular axial level. Such heterochronic grafts contributed to more posterior somites than did isochronic grafts placed at the same site, suggesting that they were not completely equivalent to the earlier streak progenitors (Tam and Tan, 1992; Cambray and Wilson, 2002). Hox expression provides an important component of the anteroposterior identity of axial cells (reviewed by Deschamps and van Nes, 2005), and can control the timing of ingression of mesodermal precursors from the epiblast (Iimura and Pourquié, 2006). It is therefore of interest to establish whether Hox gene expression is determined in axial progenitor cells.

We investigated whether LTAP populations are present in the chicken tail bud during its outgrowth. To facilitate the transplantation of defined populations of cells, we produced transgenic chickens that express the fluorescent protein GFP in every cell of the early embryo. This allowed us to follow transplanted cells temporally and to re-isolate them for transplantation to new host embryos. In a series of grafting experiments, we show that the chicken tail bud contains distinct spatially localised populations of both LTAPs and STAPs. We experimentally confirm the close similarity between the fate maps of mouse and chick tail buds, and we show that tail bud progenitor cells transplanted to earlier primitive streaks can reset their Hox identity to match their new environment.

MATERIALS AND METHODS

Viral production
The EIAV self-inactivating vector genome containing a CAG-GFP cassette was generated by digesting pCAGGS (Niwa et al., 1991) with *Sal*I and *Xho*I (blunt-ended with T4 DNA polymerase), and ligating the 1.7 kb fragment to a 0.8 kb fragment containing GFP isolated from pONY8.0G (Mazarakis et al., 2001) by digestion with *Sac*II (blunt-ended with T4 DNA polymerase) and *Hinc*II. This was inserted into the 5.4 kb pONY8.45NCZ backbone (F. J. Wilkes, J. B. Rohll, P.A.R, M. Azzouz, J. E. Miskin, F.M.E., L. E. Walmsley, N. D. Mazarakis, S. M. Kingsman and K.A.M., unpublished) following excision of the *CMV-lacZ* cassette with *Eco*RI (blunt-ended with

T4 DNA polymerase). Viral vector stocks pseudotyped with vesicular stomatitis virus glycoprotein envelope (pCMV-VSVG) were prepared using the HEK293T transient system (Lillico et al., 2007). The titer of virus [2×10^7 transducing units (TU)/ml] was estimated by the transduction of D17 cells.

Production and analysis of transgenic birds
Transgenic chickens were generated as described (McGrew et al., 2004). Eggs (39) were injected with viral vector and 16 chicks were hatched. Genomic DNA samples were obtained from CAM of chicks at hatch, and blood and semen samples from older birds. PCR analysis was carried out for the presence of proviral DNA. Eight transgenic founder birds were identified. Two founder cockerels (1-1 and 3-11) were crossed to wild-type hens and seven transgenic G_1 offspring were generated (7/511 offspring). The number and size of the proviral insertions in G_1 birds was determined by Southern blot analysis (see Fig. S1 in the supplementary material). Genomic DNA was extracted from whole blood and digested with *Eco*RI or *Stu*I. DNA was resolved on a 0.6% (w/v) agarose gel then transferred to nylon membrane (Hybond-N, Amersham Pharmacia Biotech). Membranes were hybridised with ^{32}P-labelled probes for the GFP reporter gene at 65°C, and labelled DNA detected by autoradiography. Two G_1 birds (3-11:205 and 1-1:158) were highly fluorescent, contained single-copy integrants, and were used to produce G_2 transgenic embryos. All experiments, animal breeding and care procedures were carried out under licence from the UK Home Office.

GFP expression analysis and flow cytometry
Embryos were staged according to Hamburger and Hamilton (Hamburger and Hamilton, 1951) (HH). Embryos were observed using a Leica MZFLIII florescent stereomicroscope and images captured on a Leica DC300F digital camera. For colocalisation of Hox gene expression, fluorescence was detected using laser excitation wavelengths of 488 nm and 543 nm for GFP and Alexa-Fluor 546, respectively, using an inverted confocal microscope (Nikon eC1; Nikon Instruments). Images were captured using Nikon EZ-C1 Software v3.40. Flow cytometry was performed using a Becton Dickinson FACSAria, equipped with a standard filter set, and Diva analysis software. Stage 11 HH GFP-positive embryos were dissociated using trypsin, and live cells were gated by propidium iodide exclusion. Cells from non-transgenic embryos were used to define gating parameters for GFP fluorescence expression. Data were acquired for 25,000 live events.

Immunohistochemistry and in situ hybridisation of chick embryos
For sections, embryos were isolated and fixed for 30 minutes in 4% paraformaldehyde/PBS. Tissues were cryo-embedded and sectioned at 14 μm. Sections were incubated for 30 minutes at 37°C in PBS to remove gelatin. As this treatment extinguished most of the GFP fluorescence, an Alexa-Fluor 488-conjugated rabbit anti-GFP antibody was used (Molecular Probes; 1:1000 dilution). Basement membranes were stained using rabbit anti-laminin (Sigma; 1:500 dilution). Differentiated neurons were detected with TUJ1/2 (Avance; 1:1000 dilution). Antibodies to chicken Hoxc8 (Abcam, UK) and chicken Hoxc10 were used at 1:150 and 1:20 dilutions, respectively. The antibody to Hoxc10, developed by T. Jessell, was obtained from the Developmental Studies Hybridoma Bank, University of Iowa. The secondary antibodies used were Alexa-Fluor 594-conjugated goat anti-rabbit IgG, Alexa-Fluor 594-conjugated goat anti-rabbit IgG, and Alexa-Fluor 546-conjugated goat anti-mouse IgG (Molecular Probes). Slides were counterstained with Hoechst 33342, and mounted. Whole-mount in situ hybridisation was carried out as described previously (Henrique et al., 1995). *GFP* mRNA was detected using a full-length probe to *GFP*. The riboprobe to *Hoxa10* was described by Burke et al. (Burke et al., 1995). *Hoxa10* in situ hybridisations to grafted embryos after a 1- or 8-hour incubation were performed in the same well and stained for the same period of time.

Chicken grafting experiments
CAG-GFP cockerels (Roslin Greens) were mated to wild-type hens to obtain transgenic G_2 eggs. Fertilised eggs were incubated at 38°C until the tail bud stage (26 somites, stage 15 HH). GFP-positive embryos were staged and the

caudal end of the embryo was isolated into CM1 Media (DMEM containing 10% FBS). Two dorsoventral incisions were made using tungsten needles alongside the neural tube to remove the paraxial mesoderm. A mediolateral cut was made to remove the endoderm underlying the CNH region, which was subsequently isolated. A region more caudal to this was isolated from the posterior ectoderm as ventral tail bud mesoderm (TBM). A region dorsal to this was dissected from the overlying ectoderm as the dorsal posterior tail bud (dpTB). The isolated regions were dissected into smaller pieces that were sized using a graticule. To determine the number of cells being grafted, control pieces of tissue were dissociated in trypsin and cells counted. Host embryos were inked and staged. A tungsten needle was inserted into the CNH, dpTB or ventral tail bud (vTB) regions and the tissue to be grafted was inserted into this hole. For grafts to stage 8 HH, a small incision was made just caudal to the node using a tungsten needle and the tissue to be grafted was inserted into the slit. Grafted embryos were photographed for GFP fluorescence. Grafted embryos were photographed, usually after removal of the hind limbs, and processed for in situ hybridisation or immunohistochemistry.

Mouse grafting experiments

TgN (beta-actEGFP) 04Obs (Okabe et al., 1997) ('GFP transgenic') × MF1 litters were dissected in M2 medium. The whole tail bud was isolated and the dorsoposterior tail bud was isolated using fine glass needles. First, the end of the tail was excised, and two dorsoventral longitudinal cuts made to remove the paraxial mesoderm. The ventral neurectoderm, notochord, hindgut and adjacent ventral TBM were removed by similar longitudinal cuts in the mediolateral plane. Finally, the dorsal tail bud was separated by a transverse cut posterior to the dorsal neurectoderm and the surface ectoderm was removed. Dissection of wild-type MF1 host embryos, grafts and culture were performed as described previously (Cambray and Wilson, 2002). After culture, embryo fluorescence was assessed and embryos were processed as described (Cambray and Wilson, 2007).

RESULTS

Production of GFP-expressing transgenic chickens for fate-mapping experiments

We previously reported that the CMV-IE enhancer/promoter drove limited reporter gene expression in transgenic chickens (McGrew et al., 2004). By contrast, high-level, widespread expression has been achieved using a compound CMV enhancer and a chicken β-actin promoter/intron (CAG) (Niwa et al., 1991) in several species: *Xenopus* (Sakamaki et al., 2005), mouse (Okabe et al., 1997) and axolotl (Sobkow et al., 2006). To create chickens carrying a heritable, vital marker of general utility, we constructed a lentiviral vector containing a CAG-eGFP reporter (Fig. 1A), and used this to generate two independent lines of transgenic chickens (see Materials and methods).

Transgenic G_1 cockerels were crossed to wild-type hens and the resulting embryos from incubated eggs were observed at several developmental stages. Intense GFP fluorescence was observed in CAG-GFP transgenic embryos, unlike in the previous CMV-GFP transgenic lines (see Fig. S2 in the supplementary material). GFP fluorescence was readily detected throughout the blastodermal disc in freshly laid transgenic eggs (Fig. 1B). Widespread GFP fluorescence was visible in embryos at later stages of development and section analysis confirmed its distribution throughout all tissues (Fig. 1C-G). This ubiquitous expression was verified by flow cytometric analysis of cells from dissociated day 2 (stage 11 HH) embryos. GFP fluorescence was detected in greater than 99% of the cells at this stage of development (Fig. 1I). In situ hybridisation analysis performed on day 2 (stage 14 HH) embryos additionally confirmed that the CAG-GFP transgene was actively transcribed throughout the embryo and extraembryonic regions (Fig. 1H).
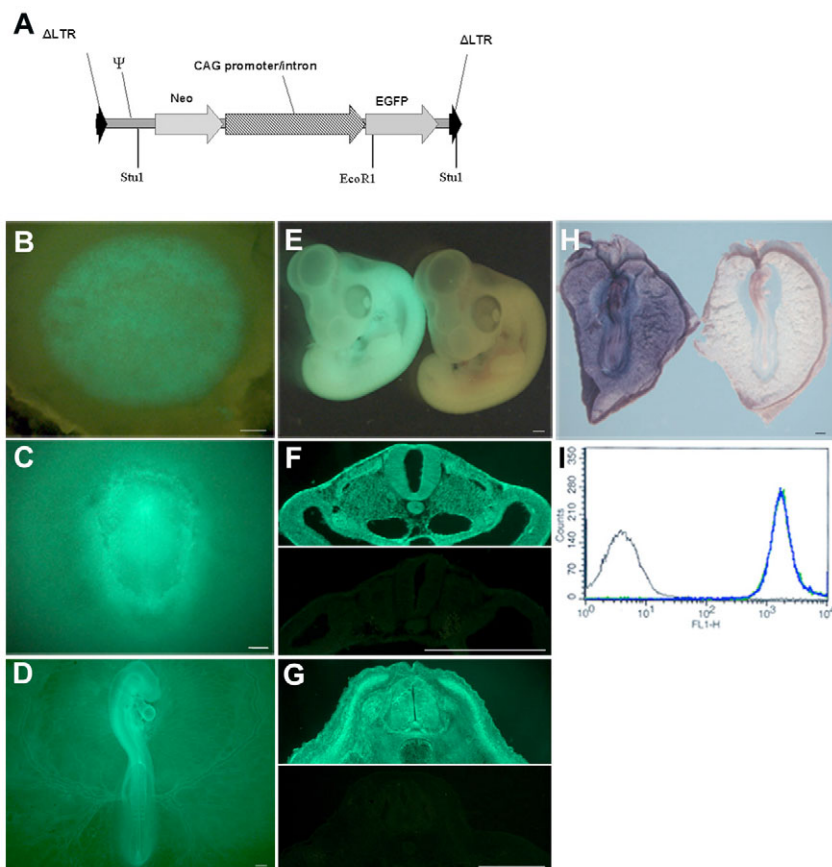
Fig. 1. GFP fluorescence in CAG-GFP transgenic chickens. (**A**) The provirus is flanked by self-inactivating LTRs (ΔLTR), and contains the virus packaging site (ψ) and a neomycin resistance open reading frame 5′ to the CAG-eGFP transgene. (**B-E**) GFP fluorescence in transgenic embryos at (B) new laid egg stage, (C) stage 4 HH, (D) stage 15 HH and (E) 5 days (transgenic on left). (**F,G**) Transverse sections of (F) stage 15 HH GFP⁺ and control embryos, and (G) day 5 GFP⁺ and control embryos. (**H**) Stage 13 HH embryos hybridised for GFP (transgenic on left). (**I**) Flow cytometric analysis of GFP fluorescence (stage 11 HH embryos). Black line, non-transgenic embryo; blue and green lines, transgenic lines 158 and 205, respectively. Scale bars: 0.5 mm.

Together, these observations indicate that the GFP reporter gene is expressed ubiquitously in embryos up to day 5 of development. Cells from these transgenic embryos are useful in grafting experiments to follow cell populations over long periods, and highly suitable for the study of putative stem cell populations. We have therefore used this line to investigate the progenitors of the anteroposterior axis in the chicken primitive streak and tail bud.

The tail bud regions of chicken and mouse embryos

In the mouse tail bud, the progenitors of the anteroposterior axis appear to fall into two categories that are spatially distinct: LTAPs that are resident in the CNH, and STAPs in the tail bud mesoderm (TBM) (Cambray and Wilson, 2002). To identify the analogous regions in the chicken, a morphological comparison of the early tail bud in mouse and chicken was carried out (Fig. 2). The nascent mouse tail bud at 10.5 days post-coitum (dpc) is morphologically similar to that of the chicken (Fig. 2B,C). The chicken tail bud stage begins with the closing of the posterior neuropore at day 2 of development [stage 13-14 HH; 19-23 somites (Schoenwolf, 1979b)]. Several hours later (stage 15 HH, ~26 somites), the posterior-ventral surface of the tail bud becomes delimited by the cloacal membrane [early tail fold stage (Schoenwolf, 1977); arrow, Fig. 2B]. This ventral tail bud boundary aided the isolation and positioning of transplanted tissues, so this stage was used for subsequent experiments. The CNH region is the area where the neural tube and notochord become indistinct from each other and from the surrounding mesoderm (Fig. 2A-B'). Staining for the extracellular matrix protein laminin identifies an area just anterior

to the CNH in mouse and chicken, where a basement membrane forms between the nascent notochord and the floorplate of the neural tube (Fig. 2B',C'). Closer morphological inspection of the posterior tail bud identifies the dorsal epithelium of the neural tube (medullary cord), which runs further posteriorly than does the CNH in both mouse and chick, eventually becoming indistinct from the TBM. This region comprises the remnant of the stem zone, which contains neural progenitor cells for the spinal cord of the tail bud (Catala et al., 1995; Delfino-Machín et al., 2005; Diez del Coral et al., 2004). A striking difference between the chicken and the mouse is the lack of laminin staining of the posterior surface ectoderm of the chicken tail bud at these stages (arrowheads, Fig. 2B',C') (Ohta et al., 2007). Ventrally, the epithelium posterior to the CNH appears to merge with loose mesenchyme of the TBM in both organisms. Therefore, the dorsoposterior tail bud (dpTB) has different characteristics from the more ventral, purely mesenchymal, ventral tail bud (vTB) region, and from the mainly epithelial CNH. The posterior tail bud has been shown to give rise to tail somites in chicken (Catala et al., 1995), but the presence of dorsoventral compartments and their capacity to act as LTAPs has not been tested in grafting assays in either organism. To address this question, we performed both isochronic and heterochronic grafts of the three tail bud regions in the chick (as indicated in Fig. 2B'): the region of the CNH where the dorsal basement membrane of the notochord will first form; a more dorsoposterior region of the tail bud posterior to the medullary cord (dpTB); and the vTB region.

The tail bud consists of at least three regions of differing fate

We first determined the normal fate of the three regions described above by homotopic, isochronic grafts in stage 15 HH embryos of GFP-positive (GFP+) transgenic cells to wild-type hosts. Host embryos were examined after 48 hours incubation (stage 24 HH). Grafts of the CNH (approximately 100-150 cells) resulted in GFP+ descendants extending from the hind limb to the tail bud in the neural tube (most prominently in the floor plate), and the paraxial mesoderm, and a few cells located in the notochord (Fig. 3B',B''; Table 1); a population of cells also remained in the CNH region (n=8/10; Fig. 3A''). Grafts of dpTB containing approximately 100-150 cells resulted in abnormally formed tail buds (n=3, data not shown). Grafts of smaller pieces of tissue (approximately 50 cells) resulted in normally patterned host embryos in which GFP+ cells were located along the body axis in a region extending from the hind limb to the tail bud (n=7/7; Fig. 3C'; Table 1), in the paraxial mesoderm (Fig. 3C''). Grafts of vTB (approximately 100-150 cells) gave rise to short stretches of paraxial mesoderm (average of six somites) and GFP+ cells did not remain in the tail bud (n=0/6; Fig. 3D',D''; Table 1).

These experiments demonstrate that the CNH contains neural and mesodermal (notochord and somite) progenitors, whereas the dpTB and vTB contain only mesodermal (somite) progenitors. The dpTB differs from the vTB, as it retains cells in the tail bud after incubation. In this respect, the dpTB behaves like the CNH, and this raises the possibility that the CNH and dpTB contain distinct types of LTAPs.

Differently fated regions show different potency on heterotopic grafting

Next, we compared the potency of the three regions by heterotopic, isochronic grafting to each of the three environments at stage 15 HH, and incubation for 48 hours, as above. Grafts to the CNH and vTB contained approximately 100-150 cells, and all grafts to the dpTB contained approximately 50 cells.
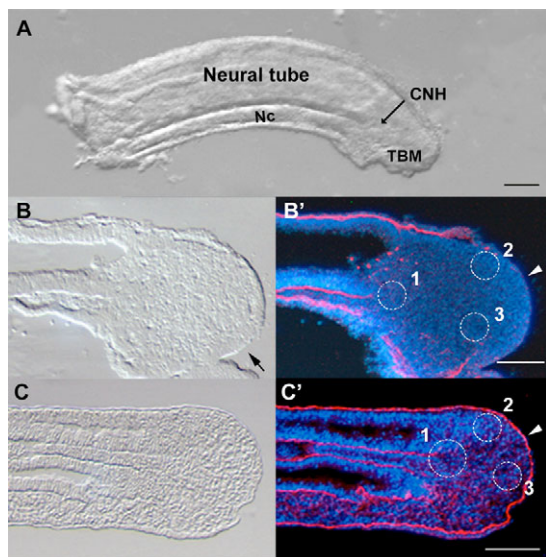
Fig. 2. The CNH region of the tail bud. (A) Caudal region of a stage 15 HH (26 somite) chicken embryo with the paraxial mesoderm removed and grafted regions indicated: Nc, notochord; CNH, chordoneural hinge; TBM, tail bud mesoderm. **(B,B′)** Mid-sagittal section of a same stage chicken embryo (B) immunostained for laminin (red in B′). Arrow, cloacal membrane; arrowhead, posterior surface ectoderm. The three grafted regions are indicated: 1, CNH; 2, dpTB; 3, ventral TB. **(C,C′)** Mid-sagittal section of a corresponding stage mouse embryo (10.5 dpc, C) immunostained for laminin (red in C′). Arrowhead, posterior surface ectoderm. Regions equivalent to those in B′ are indicated. Blue, nuclear stain. Scale bars: 0.1 mm.
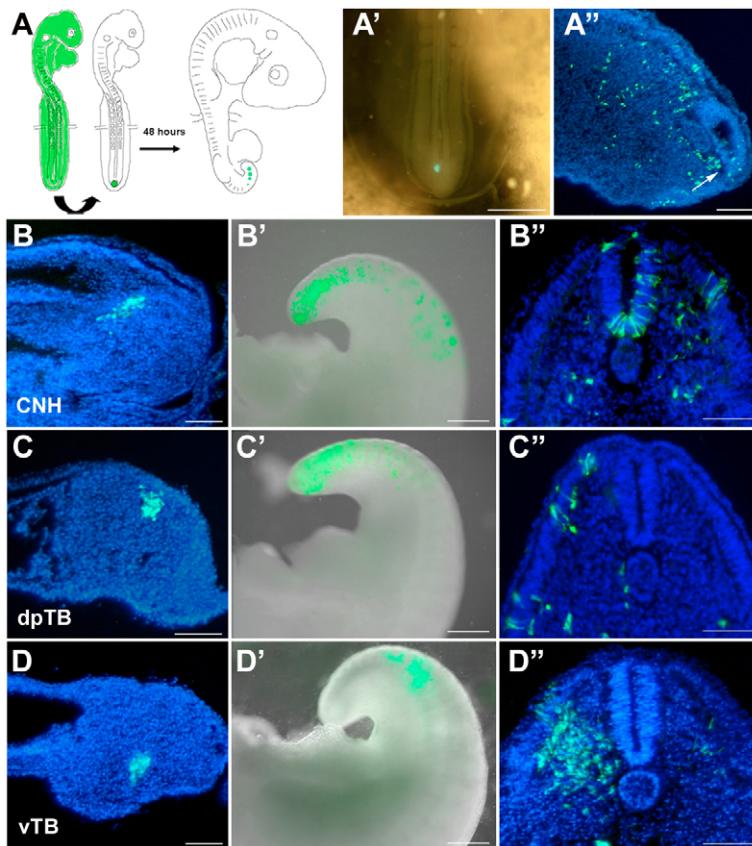
Fig. 3. Homotopic grafts in the chicken tail bud.
(**A**) CNH, dpTB or vTB regions of stage 15 HH GFP[+] embryos were grafted homotopically to host embryos and incubated for 48 hours. (**A′**) Embryo immediately after a CNH graft. (**A″**) Mid-sagittal section of a similarly grafted embryo after 48 hours (stage 24 HH). Arrow, CNH. (**B**) Mid-sagittal section of the embryo in A′ two hours after grafting. (**B′,B″**) Embryo (B′) and transverse section (B″) with a CNH graft at 48 hours. (**C**) Mid-sagittal section of an embryo with a dpTB graft two hours after grafting. (**C′,C″**) Embryo (C′) and transverse section (C″) with a dpTB graft after 48 hours. (**D**) Mid-sagittal section of an embryo with a vTB graft two hours after grafting. (**D′,D″**) Embryo (D′) and transverse section (D″) with a vTB graft after 48 hours. Blue, nuclear stain. Scale bars: A′,B,B′,C,C′,D,D′, 0.5 mm; A″,B″,C″,D″, 0.1 mm.

The CNH changed fate on grafting to the dpTB or vTB environment, such that only somitic mesoderm was produced, and GFP^{+} cells in the mesoderm were negative for the neuronal marker TUJ1 (Fig. 4A,B; Table 1). Cells were retained in the tail bud after grafting CNH to dpTB, but only approximately half of the grafts to vTB (*n*=4/7) contributed to the tail bud, suggesting that they may partially lose LTAP potency in this environment. The dpTB was not converted to a CNH-like character on grafting to the CNH, as neural descendants were almost completely absent from these grafts. Likewise, these grafts did not produce descendants in the notochord (Fig. 4C; Table 1). When grafted to the vTB, no dpTB cells were retained in the tail bud, showing that these cells lose their LTAP status in this environment (Table 1). vTB cells similarly did not contribute to the neural tube or notochord on grafting to the CNH, and neither the CNH nor the dpTB environment was able to induce their residence in the tail bud (Fig. 4E,F; Table 1). Instead, these grafts gave rise to short stretches of somitic mesoderm. Similarly, grafts of posterior presomitic mesoderm to the CNH region generated short tracts of somitic mesoderm (*n*=6/6) (data not shown). Together with the fate mapping studies above, these results suggest that: (1) the CNH is adaptable to new environments but is less likely to lose LTAP status than the dpTB; (2) the dpTB is more limited in its potency to produce multiple axial derivatives than the CNH, and readily loses LTAP status in the vTB environment; and (3) the vTB does not have long-term axial progenitor potency.

Tail bud progenitor cells repopulate the tail bud after heterochronic transplantations to early somite stage embryos

The ability of both CNH and dpTB to retain cells in the tail bud after homotopic transplantation suggests that both populations are LTAPs. As mouse LTAPs have the ability to contribute to the axis and tail

**Table 1. Homotopic and heterotopic grafts in the chicken tail bud**

Donor	Graft site	Embryos grafted	Neural tube	Notochord	Paraxial mesoderm	Tail bud
CNH	CNH	10	6	4*	10	8
	dpTB	7	1	0	7	6
	vTB	7	1	1	6	4
dpTB	CNH	10	1[†]	0	10	9
	dpTB	7	0	0	7	7
	vTB	7	0	0	7	1
vTB	CNH	6	0	0	6	0
	dpTB	6	0	0	6	0
	vTB	6	0	0	6	0

Contribution of GFP^{+} grafted cells to tissues of host embryos 48 hours after grafting (shading indicates homotopic grafts).
*A few scattered cells.
[†]Very few cells (*n*=2).
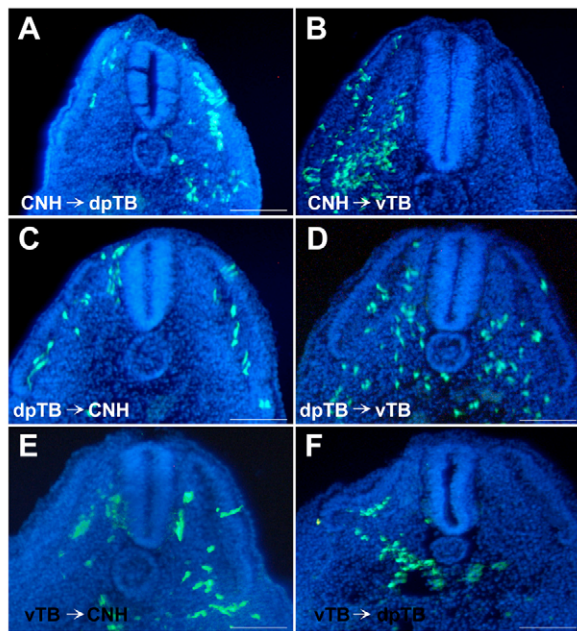
Fig. 4. Heterotopic grafts in the chicken tail bud. (A-F) Transverse sections of host embryos 48 hours after grafting of the CNH to (A) the dpTB or (B) the vTB; the dpTB to (C) the CNH or (D) the vTB; and the vTB to (E) the CNH or (F) the dpTB. Blue, nuclear stain. Scale bars: 0.1 mm.

bud after heterochronic transplantation, we performed this assay using chick stage 15 HH CNH and dpTB. Grafts (approximately 50 cells) were placed immediately caudal to the node region of stage 8 HH embryos (Fig. 5B,B'), which were then incubated for 48 hours (stage 20 HH). Isochronic grafts of GFP$^+$ tissue in this region

showed extensive contribution to the body axis. GFP$^+$ cells were located in paraxial mesoderm and the neural tube from the forelimb level to the tail bud ($n=5/6$; Fig. 5C,C'). These results are consistent with the fate map of the chicken posterior node region (Catala et al., 1996; Psychoyos and Stern, 1996; Charrier et al., 1999; Freitas et al., 2001). Heterochronic grafts of either stage 15 HH CNH ($n=11/11$) or dpTB ($n=5/5$) resulted in a long stretch of GFP$^+$ cells along the body axis, running from the forelimb level to the tail bud (Fig. 5D,E). The CNH contributed cells to neurectoderm and paraxial mesoderm, similar to homotopic grafts (Fig. 5D'), whereas descendants of the dpTB were found exclusively in the paraxial mesoderm (Fig. 5E'). By contrast, grafts of vTB contributed cells to a short series of somites along the body axis and did not repopulate the tail bud ($n=4/5$; Fig. 5F,F'). These experiments demonstrate that both the CNH and dpTB appear to act as LTAPs in heterochronic graft assays. We tested whether the structural equivalent of the dpTB in the mouse (Fig. 2C') also contains apparent LTAPs with exclusively somitic potential. GFP$^+$ tissue from this region was grafted to the node/streak border of E8.5 (3-5 somite) mouse embryos and cultured for 48 hours in vitro. GFP$^+$ cells contributed exclusively to somites, and in the tail bud were found in the TBM, not the CNH ($n=6/6$; see Fig. S3A,B in the supplementary material). Therefore, a similar population to the chick dpTB exists in mouse.

The CNH region of the tail bud can be serially transplanted between embryos

A more stringent test of LTAP status is to serially graft cells from the tail bud of host embryos to examine their ability to contribute to the same axial stretch more than once, as well as their capacity for retention in the tail bud over multiple passages (Fig. 6A). The CNH region from stage 15 HH GFP$^+$ embryos was isolated and transplanted to stage-matched host embryos, as above. Embryos were incubated for 20 hours (stage 20 HH). After incubation, the CNH regions were re-isolated and grafted into new stage 15 HH
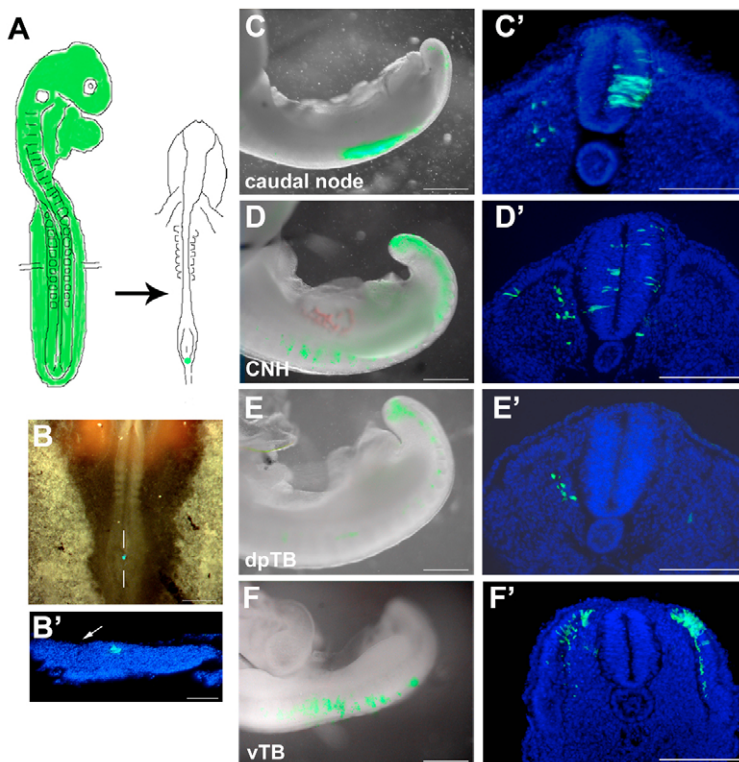
Fig. 5. Heterochronic transplantation of tail bud regions to early embryos. (**A**) Tissue caudal to the node or tail bud regions from stage 15 HH embryos were grafted into 6-somite (stage 8 HH) hosts and incubated for 48 hours. (**B**) An embryo immediately after grafting. Line indicates level of the section. (**B'**) Mid-sagittal section of host embryo two hours after grafting. Arrow, Hensen's node. (**C-F'**) Embryos and transverse sections 48 hours after (C,C') homotopic graft of caudal node tissue; (D,D') heterochronic graft of CNH; (E,E') heterochronic graft of the dpTB; (F,F') heterochronic graft of the vTB. Blue, nuclear stain. Scale bars: B,C,D,E, 0.5 mm; C',D',E', 0.1 mm.

hosts that were incubated for 20 hours. The isolation and grafting of GFP^{+} cells in the CNH region was repeated for a third time and the host embryos were incubated for 48 hours (stage 24 HH). GFP^{+} cells were found in the CNH of the tail bud (n=4), although fewer labeled cells were present in the CNH after successive grafts (Fig. 6B,C,D). Some graft-derived GFP^{+} cells and their host-derived neighbours were positive for the neural marker TUJ1, suggesting that they were neural crest derivatives. As neural crest is derived from dorsal neural tube, it is likely that these cells were incorporated into the neural
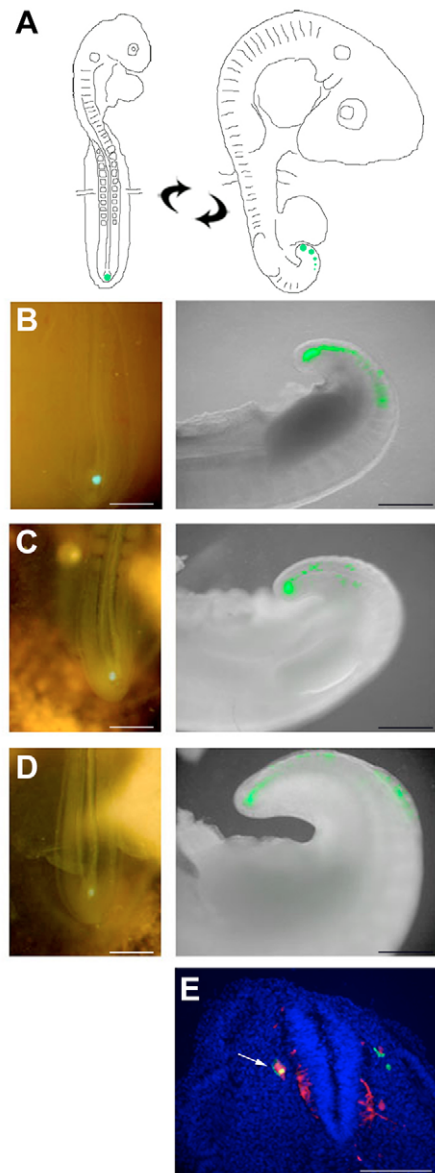

Fig. 6. Serial transplantation of the CNH. (**A**) Serial grafting experiments between stage 15 HH and stage 20 HH embryos. (B-D) Embryos immediately after grafting (left) and after incubation (right). (**B**) CNH from a stage 15 HH GFP[+] embryo grafted to a host embryo and incubated for 20 hours. (**C**) CNH region from the first host was grafted to a stage 15 HH host and incubated for 20 hours. (**D**) CNH region from the second host was grafted to a stage 15 HH host and incubated for 48 hours. (**E**) Transverse section of the third host embryo immunostained for the neuronal marker TUJ1 (red), which labels some GFP^{+} cells (arrow). Blue, nuclear stain. Scale bars: B-D, 0.5 mm; E, 0.1 mm.

tube after being grafted dorsally into the host tail bud. GFP^{+} cells in the final host embryos were found only in paraxial mesoderm or neural derivatives (Fig. 6E, data not shown). Although some cells integrated correctly (Fig. 6E), the morphology of the tissue formed from the GFP^{+} cells in the third host was often aberrant, with ectopic somites forming dorsally (data not shown). Serial grafts were also carried out using the dpTB as a donor. These grafts differed from CNH grafts in that GFP^{+} cells were retained in the tail bud only for the first two passages through host embryos (n=3/3, data not shown). The CNH of the chicken is thus similar to the mouse CNH in that it can be serially passaged between host embryos, producing both differentiated axial and tail bud progenitors on each passage, but dpTB cannot repopulate the tail bud indefinitely. Furthermore, the CNH has both greater potency, in terms of the number of tissue types it can produce, and greater LTAP capacity, in terms of the number of times it can repopulate the tail bud, than the dpTB.

The Hox identity of tail bud progenitor cells is not determined

The contribution of tail bud cells to anterior axial tissues in heterochronic grafts suggests that their anteroposterior identity is not fixed. This identity is in part determined by the expression of specific Hox genes. To test whether the expression of Hox genes in grafted cells conforms to that of the host, we analysed the expression of selected Hox genes in grafted embryos at different time points after transplantation. *Hoxa10* mRNA is absent in the embryo at stages 8-10 HH, but is expressed in the tail bud, including the CNH region, of stage 15 HH embryos (Fig. 7A). One day later (stage 20 HH), *Hoxa10* expression extends caudally from somite 25 to the tail bud (Burke et al., 1995; Dubrulle et al., 2001) (Fig. 7D′). The protein of a paralogous Hox gene, *Hoxc10*, is also present in the CNH, dpTB and TBM of stage 15 HH embryos (Fig. 7A′). No expression was detected immediately anterior to the CNH in the forming notochord.
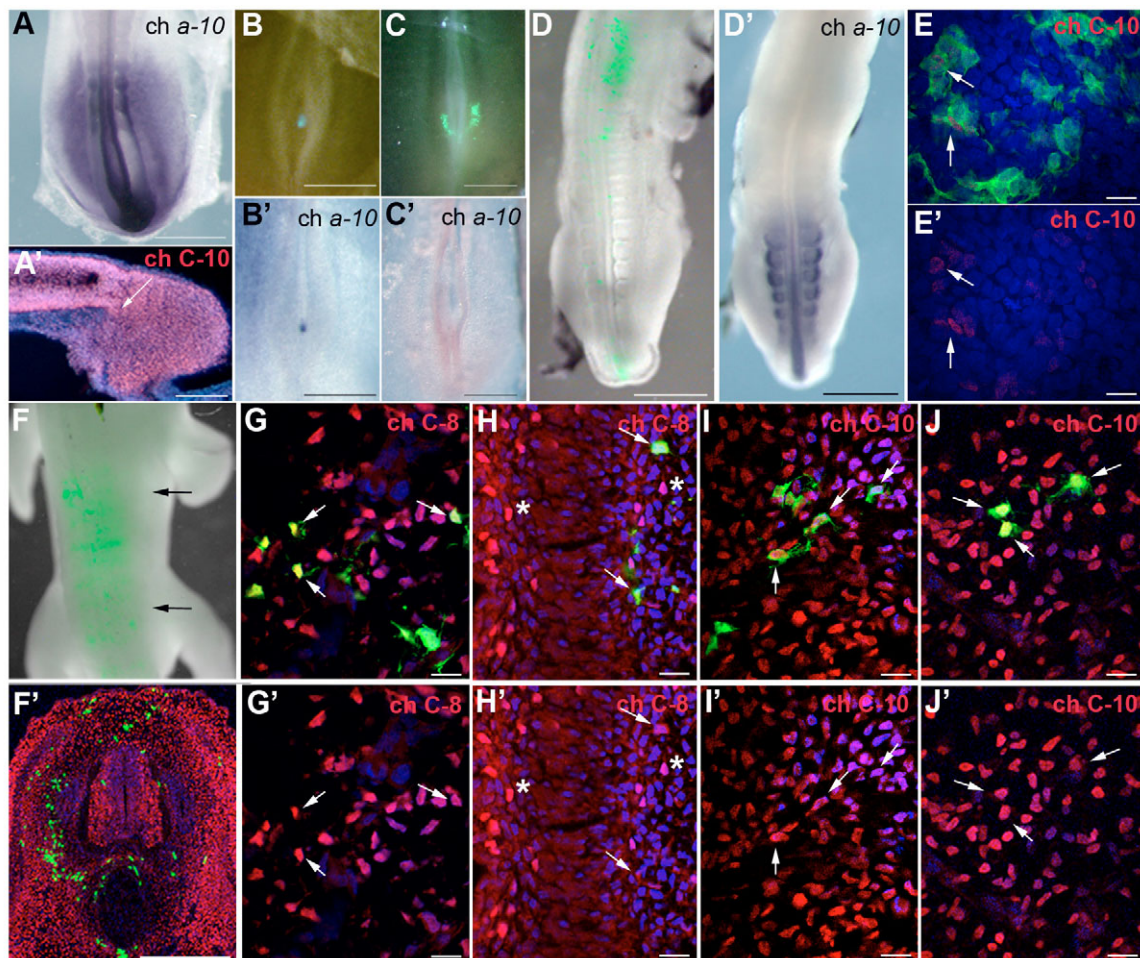
We investigated whether the progenitor cell populations of the tail bud maintained their Hox gene expression pattern when challenged by heterochronic grafting of stage 15 HH CNH or dpTB to the caudal node region of stage 8 HH embryos, as above (Fig. 5). In situ hybridisation analysis shortly after grafting confirmed that the grafted tissue expressed *Hoxa10* (n=7/7; Fig. 7B,B′). However, after an 8-hour incubation, the grafted tissue, like the surrounding host tissue, did not have detectable signal for *Hoxa10* (n=9/10; Fig. 7C,C′). After 48 hours, no ectopic anterior *Hoxa10* expression was observed in grafted embryos in cells derived from either CNH or dpTB grafts (n=9/9; Fig. 7D,D′). Immunostaining for Hoxc10 protein in similarly grafted embryos after 48 hours revealed that the majority of anterior GFP^{+} cells were no longer positive for this protein, although a few cells, generally in small clusters, showed some staining (Fig. 7E,E′). All Hoxc10 labeling was lost in anterior GFP^{+} cells after four days of incubation (data not shown). GFP^{+} cells in the posterior hindlimb region, as in control isochronic grafted embryos, were Hoxc10 positive (Fig. 7I-J'), like their wild-type neighbours. Therefore, the expression of posterior Hox genes in tail bud progenitor cells is downregulated shortly after transplant to an anterior environment in which these genes are not expressed. Expression is then correctly activated in posterior, but not anterior, graft derivatives.

To determine whether graft-derived cells in the anterior part of the axis were capable of expressing any Hox gene correctly, we tested whether these cells expressed a more anterior Hox gene, Hoxc8. Hoxc8 protein is first detected in the neural tube and the surrounding paraxial mesoderm in the brachial region (~somite 22) at stage 21-24 HH (Belting et al., 1998) (Fig. 7F′). In control isochronic grafts

Fig. 7. Hox identity is not determined in tail bud progenitor cells. (**A**) Tail bud (stage 15 HH) hybridised for *Hoxa10*. (**A'**) Mid-sagittal section (stage 16 HH) immunostained for Hoxc10. Arrow indicates the CNH. (**B-D'**) CNH or dpTB regions (stage 15 HH) grafted into stage 8 HH hosts. In situ hybridisations were carried out for *Hoxa10*. (B,B') One hour incubation. GFP$^+$ tissue expresses *Hoxa10*. Eight- (C,C') or 48 (D,D')-hour incubations. Anterior GFP$^+$ tissue is negative for *Hoxa10*. (**E,E'**) Anterior transverse section from a similarly grafted embryo after 48 hours, immunostained for Hoxc10. Arrows indicate Hoxc10 positive GFP$^+$ cells. (**F-J'**) Whole-mount (F) and transverse sections (F'-J') of an embryo grafted as in B-D and incubated for four days (stage 25 HH). Transverse sections at the level of the anterior arrow were immunostained for Hoxc8 (F'-H'), and those at the level of the posterior arrow with a Hoxc10 antibody (I-J'). Anterior sections from embryos after (G,G') a homotopic caudal node graft or (H,H') a heterochronic CNH graft, immunostained for Hoxc8. Arrows indicate Hoxc8-positive GFP$^+$ cells; asterisks indicate Hoxc8-positive host cells. Posterior sections after (I,I') a homotopic caudal node graft or (J,J') a heterochronic CNH graft, immunostained for Hoxc10. Arrows indicate Hoxc10-positive GFP$^+$ cells. Blue, nuclear stain. Scale bars: A,B,B'-D', 0.5 mm; A', 0.1 mm; F', 250 µm; E,E',G-I', 30 µm.

of GFP$^+$ tissue to the anterior node region, GFP$^+$ cells located in anterior Hoxc8-expressing regions were Hoxc8 positive (Fig. 7G,G'). Heterochronic grafts, performed as above, were incubated for four days (stage 24 HH) and then GFP$^+$ cells in the paraxial mesoderm at this axial level were examined for the presence of Hoxc8 protein. GFP$^+$ cells located in anterior Hoxc8-expressing regions contained detectable Hoxc8 (*n*=5 embryos, Fig. 7H,H'). Together, these experiments show that tail bud progenitor cells can reset their Hox gene expression to match that of their surrounding tissue.

DISCUSSION
Our production of a new transgenic line expressing ubiquitous GFP has enabled us to demonstrate that the chicken tail bud contains localised axial progenitors in the CNH, dpTB and vTB, each with different properties. Cells in the CNH are fated to produce neural and mesodermal descendants, and this relies on the CNH

environment. Cells in the dpTB of the chicken and mouse constitute a mesodermal progenitor cell population, which, even in the CNH environment, do not produce neural derivatives. This population also differs from the CNH in that fewer cells are retained in the tail bud after serial transplantations. Cells of the vTB are not resident in the tail bud. Although CNH and dpTB populations express anteroposterior level-specific Hox genes, this expression profile can be changed in the context of a more anterior node/primitive streak environment. Thereafter, CNH and dpTB descendants express appropriate Hox genes for their axial level.

A new tool for avian fate mapping
Seminal research by Le Douarin and colleagues was facilitated by the development and use of quail-chick chimeras for fate mapping experiments (Le Douarin, 1969). Detection of graft derivatives requires fixation of the specimens. Electroporation and infection using viruses allows transient expression of vital markers, such as

GFP (reviewed by Ishii and Mikawa, 2005), but these techniques are unable to produce long-term heritability of the marker gene. Lentiviral vectors were recently used to generate germ line transgenic chickens with high efficiency, including a line incorporating a CMV-GFP transgene, which showed very limited expression in embryos (McGrew et al., 2004) (see Fig. S2 in the supplementary material). The CAG-GFP transgene described here drives ubiquitous expression of GFP during chicken embryogenesis, at higher levels than in a previously described line of transgenic chickens (Chapman et al., 2005). This CAG-GFP line will be a powerful resource for investigations in the chicken requiring tracking of cells in vivo over long periods.

Progenitor populations in the tail bud

Our data support and extend previous research demonstrating that a resident population of LTAPs is located in the CNH of the mouse tail bud using heterochronic grafts to early somite stage embryos (Cambray and Wilson, 2002). By comparing chick and mouse dpTB in this study, we complete these data to show a highly similar organisation of progenitors, despite some differences in tail bud morphology. Only heterochronic grafts were possible in the mouse to test the capacity of tail bud regions to act as long-term progenitors, because mouse embryos can be manipulated and cultured for only a limited period. In the chick it has been possible to perform both heterochronic and isochronic grafts, and thus to extend the findings from mouse. The fact that the pattern of axial tissue and tail bud contribution is very similar whether grafts are isochronic or heterochronic suggests a continuity of cell functions over long periods of axis elongation. This correlates well with the expression of primitive streak markers in tail bud regions, and indeed in several organisms it has already been noted that the gene expression patterns highlight a structural continuity between the primitive streak, or its equivalent, and the tail bud (Delfino-Machín et al., 2005; Cambray and Wilson, 2007). These expression studies also show that the dpTB expresses markers characteristic of the primitive streak. As primitive streak and dpTB share the property that they produce mesoderm exclusively, even when transplanted to a region that produces neural and notochord derivatives (Cambray and Wilson, 2007) (Fig. 5, Table 1), this molecular similarity between the streak and tail bud also correlates with a functional continuity.

At least early on, the node region can give rise to cells in the primitive streak (Forlani et al., 2003). We have observed that the CNH can give rise to cells in the dpTB after homotopic grafting (data not shown), but the converse was not seen. Therefore, at least some dpTB cells may derive from the CNH, raising the possibility that CNH cells are a more primitive progenitor type than are the dpTB cells. This is supported by the low potential of cells of the dpTB to remain in the tail bud following multiple passages. Our experiments, because they deal with populations rather than single cells, are not informative about the progression of lineage restriction in these tail bud domains, and, in particular, cannot distinguish between multipotent progenitors in the CNH and several lineage-restricted populations.

Retrospective lineage analysis in the mouse suggests that axial progenitor cells are restricted in their contribution to the somite along the mediolateral axis (Eloy-Trinquet and Nicolas, 2002). In our experiments, homotopic grafts in the tail bud produced GFP[+] descendants bilaterally in both the medial and lateral compartments of the somite. However, homotopic grafts of the CNH and dpTB gave rise to a greater proportion of GFP^{+} cells in medial somitic derivatives than did grafts to the vTB (Figs 3, 4). Cells placed heterotopically in the CNH or heterochronically in the node generally contributed to the medial somitic compartment, demonstrating that cells destined for lateral somitic regions (i.e. vTB cells) are constrained by the CNH to exit to medial locations (see Fig. 5C′-F′; see Fig. S3 in the supplementary material). As the CNH is mostly composed of node/streak border derivatives that exit this region to medial somite regions (Selleck and Stern, 1991; Selleck and Stern, 1992; Catala et al., 1996; Psychoyos and Stern, 1996; Charrier et al., 1999; Freitas et al., 2001; Cambray and Wilson, 2007; Iimura and Pourquié, 2007), this pattern of exit is also strikingly conserved through axis elongation. It is not certain whether the progenitors of lateral somitic regions are also LTAPs in an, as yet, untested region, or whether the short-term contributing cells in the vTB make up the bulk of lateral somite progenitors.

Hox identity is plastic in tail bud progenitor cells

We demonstrate that Hox gene expression is not determined in progenitor cells in the tail bud. Hox identity in the paraxial mesoderm is known to become fixed before somite formation (Kieny et al., 1972; Nowicki and Burke, 2000; Omelchenko and Lance-Jones, 2003). Similarly, Iimura and Pourquié observed the maintenance of *Hoxb9* expression in primitive streak cells at a 6-hour timepoint after transplant to a younger streak not expressing *Hoxb9* (Iimura and Pourquié, 2006), suggesting that these cells retain their anteroposterior identity. It is possible that our timepoint (8 hours) just bypasses this period, or that the size of the graft is crucial for downregulation owing to cell contact with non-expressing neighbours. The latter phenomenon has been observed with Hox-expressing cells in the hindbrain, where clumps of heterotopically grafted cells maintained their Hox expression profile, while those that became isolated from the main clump and were surrounded with non-expressing cells downregulated Hox expression (Trainor and Krumlauf, 2000). We observed some residual *Hoxc10* expression several days after transplantation, associated with clumps of GFP^{+} cells rather than dispersed cells (Fig. 7D), indicating that cell-cell interactions may be important in maintaining or modulating Hox gene expression. Interestingly, Iimura and Pourquié proposed that activation of sequentially more posterior Hox genes in subsets of epiblast cells retards their ingression, providing a mechanism to control the timing of cell ingression through the streak (Iimura and Pourquié, 2006). If such a mechanism is used, it is unlikely to act by activating Hox expression cell-autonomously, as our data show that the Hox identity of axial progenitor cells is influenced by neighbouring cells.

We have provided molecular evidence that LTAP populations at tail bud stages have more posterior identities than at earlier stages, confirming that in vivo these cells do not 'self-renew', i.e. give rise to exact copies of themselves. However, their interpretation of anterior cues by changes in Hox gene expression suggests that under certain conditions they have the potential to self-renew.

References
Belting, H. G., Shashikant, C. S. and Ruddle, F. H. (1998). Modification of expression and cis-regulation of Hoxc8 in the evolution of diverged axial morphology. *Proc. Natl. Acad. Sci. USA* **95**, 2355-2360.

Brown, J. M. and Storey, K. G. (2000). A region of the vertebrate neural plate in which neighbouring cells can adopt neural or epidermal fates. *Curr. Biol.* **10**, 869-872.

Burke, A. C., Nelson, C. E., Morgan, B. A. and Tabin, C. (1995). Hox genes and the evolution of vertebrate axial morphology. *Development* **121**, 333-346.

Cambray, N. and Wilson, V. (2002). Axial progenitors with extensive potency are localised to the mouse chordoneural hinge. *Development* **129**, 4855-4866.

Cambray, N. and Wilson, V. (2007). Two distinct sources for a population of maturing axial progenitors. *Development* **134**, 2829-2840.

Catala, M., Teillet, M.-A. and Le Douarin, N. M. (1995). Organization and development of the tail bud analyzed with the quail-chick chimaera system. *Mech. Dev.* **51**, 5l-65.

Catala, M., Teillet, M.-A., De Robertis, E. M. and Le Douarin, N. M. (1996). A spinal cord fate map in the avian embryo: while regressing, Hensen's node lays down the notochord and floor plate thus joining the spinal cord lateral walls. *Development* **122**, 2599-2610.

Chapman, S. C., Lawson, A., Macarthur, W. C., Wiese, R. J., Loechel, R. H., Burgos-Trinidad, M., Wakefield, J. K., Ramabhadran, R., Mauch, T. J. and Schoenwolf, G. C. (2005). Ubiquitous GFP expression in transgenic chickens using a lentiviral vector. *Development* **132**, 935-940.

Charrier, J. B., Teillet, M.-A., Lapointe, F. and Le Douarin, N. M. (1999). Defining subregions of Hensen's node essential for caudalward movement, midline development and cell survival. *Development* **126**, 4771-4783.

Criley, B. B. (1969). Analysis of embryonic sources and mechanims of development of posterior levels of chick neural tubes. *J. Morphol.* **128**, 465-501.

Davis, R. L. and Kirschner, M. W. (2000). The fate of cells in the tailbud of Xenopus laevis. *Development* **127**, 255-267.

Delfino-Machín, M., Lunn, J. S., Breitkreuz, D. N., Akai, J. and Storey, K. G. (2005). Specification and maintenance of the spinal cord stem zone. *Development* **132**, 4273-4283.

Deschamps, J. and van Nes, J. (2005). Developmental regulation of the Hox genes during axial morphogenesis in the mouse. *Development* **132**, 2931-2942.

Diez del Corral, R. and Storey, K. G. (2004). Opposing FGF and retinoid pathways: a signalling switch that controls differentiation and patterning onset in the extending vertebrate body axis. *BioEssays* **26**, 857-869.

Dubrulle, J., McGrew, M. J. and Pourquie, O. (2001). FGF signaling controls somite boundary position and regulates segmentation clock control of spatiotemporal Hox gene activation. *Cell* **106**, 219-232.

Eloy-Trinquet, S. and Nicolas, J. F. (2002). Cell coherence during production of the presomitic mesoderm and somitogenesis in the mouse embryo. *Development* **129**, 3609-3619.

Forlani, S., Lawson, K. A. and Deschamps, J. (2003). Acquisition of Hox codes during gastrulation and axial elongation in the mouse embryo. *Development* **130**, 3807-3819.

Freitas, C., Rodrigues, S., Charrier, J. B., Teillet, M. A. and Palmeirim, I. (2001). Evidence for medial/lateral specification and positional information within the presomitic mesoderm. *Development* **28**, 5139-5147.

Gaertner, R. A. (1949). Development of the posterior trunk and tail of the chicken embryo. *J. Exp. Zool.* **111**, 157-174.

Gofflot, F., Hall, M. and Morriss-Kay, G. M. (1997). Genetic patterning of the developing mouse tail at the time of posterior neuropore closure. *Dev. Dyn.* **210**, 431-445.

Gont, L. K., Steinbeisser, H., Blumbergand, B. and De Robertis, E. M. (1993). Tail formation as a continuation of gastrulation: the multiple cell populations of the Xenopus tailbud derive from the late blastopore lip. *Development* **119**, 991-1004.

Greco, T. L., Takada, S., Newhouse, M. M., McMahon, J. A., McMahon, A. P. and Camper, S. A. (1996). Analysis of the vestigial tail mutation demonstrates that Wnt-3a gene dosage regulates mouse axial development. *Genes Dev.* **10**, 313-324.

Hamburger, V. and Hamilton, H. L. (1951). A series of normal stages in the development of the chick embryo. *J. Morphol.* **88**, 49-92.

Henrique, D., Adam, J., Myat, A., Chitnis, A., Lewis, J. and Ish-Horowicz, D. (1995). Expression of a Delta homologue in prospective neurons in the chick. *Nature* **375**, 787-790.

Herrmann, B. G., Labeit, S., Poustka, A., King, T. R. and Lehrach, H. (1990). Cloning of the T gene required in mesoderm formation in the mouse. *Nature* **343**, 617-622.

Homdahl, D. E. (1925). Experimentelle Untersuchungen iiber die lage der grenze zwischen primarer und sekundarer korperentwicklung beim huhn. *Anat. Anz.* **59**, 393-396.

Iimura, T. and Pourquié, O. (2006). Collinear activation of Hoxb genes during gastrulation is linked to mesoderm cell ingression. *Nature* **442**, 568-571.

Iimura, T., Yang, X., Weijer, C. J. and Pourquié, O. (2007). Dual mode of paraxial mesoderm formation during chick gastrulation. *Proc. Natl. Acad. Sci. USA* **104**, 2744-2749.

Ishii, Y. and Mikawa, T. (2005). Somatic transgenesis in the avian model system. *Birth Defects Res. C. Embryo Today* **75**, 19-27.

Kanki, J. P. and Ho, R. K. (1997). The development of the posterior body in zebrafish. *Development* **124**, 881-893.

Kieny, M., Mauger, A. and Sengel, P. (1972). Early regionalization of somitic mesoderm as studied by the development of axial skeleton of the chick embryo. *Dev. Biol.* **28**, 142-161.

Kilka, E. and Jelinek, R. (1969). The structure of the end and tail bud of the chick embryo. *Folia Morphol. Praha* **17**, 29-40.

Knezevic, V., De Santo, R. and Mackem, S. (1998). Continuing organizer function during chick tail development. *Development* **125**, 1791-1801.

Lanot, R. (1980). Régression de l'intestin caudal et phénomenes associés chez l'embryon de poulet. *Arch. Anat. Microsc. Morphol. Exp.* **69**, 243-257.

Lawson, K. A., Meneses, J. J. and Pedersen, R. A. (1991). Clonal analysis of epiblast fate during germ layer formation in the mouse embryo. *Development* **113**, 891-911.

Le Douarin, N. M. (1969). Particularités du noyau interphasique chez la Caille japonaise (Coturnix coturnix japonica). Utilisation de ces particularités comme 'marquage biologique' dans les recherches sur les interactions tissulaires et les migrations cellulaires au cours de l'ontogénèse. *Bull. Biol. Fr. Belg.* **103**, 435-452.

Lillico, S. G., Sherman, A., McGrew, M. J., Robertson, C. D., Smith, J., Haslam, C., Barnard, P., Radcliffe, P. A., Mitrophanous, K. A., Elliot, E. A. et al. (2007). Oviduct-specific expression of two therapeutic proteins in transgenic hens. *Proc. Natl. Acad. Sci. USA* **104**, 1771-1776.

Marlow, F., Gonzalez, E. M., Yin, C., Rojo, C. and Solnica-Krezel, L. (2004). No tail co-operates with non-canonical Wnt signaling to regulate posterior body morphogenesis in zebrafish. *Development* **131**, 203-216.

Mathis, L. and Nicolas, J. F. (2000). Different clonal dispersion in the rostral and caudal mouse central nervous system. *Development* **127**, 1277-1290.

Mazarakis, N. D., Azzouz, M., Rohll, J. B., Ellard, F. M., Wilkes, F. J., Olsen, A. L., Carter, E. E., Barber, R. D., Baban, D. F., Kingsman, S. M. et al. (2001). Rabies virus glycoprotein pseudotyping of lentiviral vectors enables retrograde axonal transport and access to the nervous system after peripheral delivery. *Hum. Mol. Genet.* **10**, 2109-2121.

McGrew, M. J., Sherman, A. S., Ellard, F. M., Lillico, S. G., Gilhooley, H. J., Mitrophanous, K. A., Kingsman, A. J. and Sang, H. (2004). Efficient production of germline transgenic chickens using lentiviral vectors. *EMBO Rep.* **5**, 728-733.

Miller, S. A. and Briglin, A. (1996). Apoptosis removes chick embryo tail gut and remnant of the primitive streak. *Dev. Dyn.* **206**, 212-218.

Nicolas, J. K., Mathis, L. and Bonnerot, C. (1996). Evidence in the mouse for self-renewing stem cells in the formation of a segmented longitudinal structure, the myotome. *Development* **122**, 2933-2946.

Niwa, H., Yamamura, K. and Miyazaki, J. (1991). Efficient selection for high-expression transfectants with a novel eukaryotic vector. *Gene* **108**, 193-199.

Nowicki, J. L. and Burke, A. C. (2000). Hox genes and morphological identity: axial versus lateral patterning in the vertebrate mesoderm. *Development* **127**, 4265-4275.

Ohta, S., Suzuki, K., Tachibana, K., Tanaka, H. and Yamada, G. (2007). Cessation of gastrulation is mediated by suppression of epithelial-mesenchymal transition at the ventral ectodermal ridge. *Development* **134**, 4315-4324.

Okabe, M., Ikawa, M., Kominami, K., Nakanishi, T. and Nishimune, Y. (1997). 'Green mice' as a source of ubiquitous green cells. *FEBS Lett.* **407**, 313-319.

Omelchenko, N. and Lance-Jones, C. (2003). Programming neural Hoxd10: in vivo evidence that early node-associated signals predominate over paraxial mesoderm signals at posterior spinal levels. *Dev. Biol.* **261**, 99-115.

Pasteels, J. (1943). Proliférations et croissance dans la gastrulation et la formation de la queue des Vertébrés. *Arch. Biol.* **54**, 2-51.

Psychoyos, D. and Stern, C. D. (1996). Fates and migratory routes of primitive streak cells in the chick embryo. *Development* **122**, 1523-1534.

Roszko, I., Faure, P. and Mathis, L. (2007). Stem cell growth becomes predominant while neural plate progenitor pool decreases during spinal cord elongation. *Dev. Biol.* **304**, 232-245.

Sakamaki, K., Takagi, C., Yoshino, J., Yokota, H., Nakamura, S., Kominami, K., Hyodo, A., Takamune, K., Yuge, M. and Ueno, N. (2005). Transgenic frogs expressing the highly fluorescent protein venus under the control of a strong mammalian promoter suitable for monitoring living cells. *Dev. Dyn.* **233**, 562-569.

Sanders, E. J., Khare, M. K., Ooi, V. C. and Bellairs, R. (1986). An experimental and morphological analysis of the tail bud mesenchyme of the chick embryo. *Anat. Embryol.* **174**, 179-185.

Schoenwolf, G. C. (1977). Tail (end) bud contributions to the posterior region of the chick embryo. *J. Exp. Zool.* **210**, 227-246.

Schoenwolf, G. C. (1979a). Histological and ultrastructural observations of tail bud formation in the chick embryo. *Anat. Rec.* **193**, 131-147.

Schoenwolf, G. C. (1979b). Observations on closure of the neuropores in the chick embryo. *Am. J. Anat.* **155**, 445-465.

Schoenwolf, G. C. (1981). Morphogenetic processes involved in the remodeling of the tail region of the chick embryo. *Anat. Embryol.* **162**, 183-197.

Schoenwolf, G. C. and Delongo, J. (1980). Ultrastructure of secondary neurulation in the chick embryo. *Am. J. Anat.* **158**, 43-63.

Seichert, V. and Jelínek, R. (1968). Tissue shifts in the end and tail bud of the chick embryo. *Folia Morphol. Praha* **16**, 436-446.

Selleck, M. A. and Stern, C. D. (1991). Fate mapping and cell lineage analysis of Hensen's node in the chick embryo. *Development* **112**, 615-626.

Selleck, M. A. and Stern, C. D. (1992). Evidence for stem cells in the mesoderm of Hensen's node and their role in embryonic pattern formation. In *Formation and Differentiation of Early Embryonic Mesoderm* (ed. R. Bellairs, E. J. Sanders and J. W. Lash), pp. 23-31. New York: Plenum Press.

Sobkow, L., Epperlein, H. H., Herklotz, S., Straube, W. L. and Tanaka, E. M. (2006). A germline GFP transgenic axolotl and its use to track cell fate: dual origin of the fin mesenchyme during development and the fate of blood cells during regeneration. *Dev. Biol.* **290**, 386-397.

Stern, C. D., Charité, J., Deschamps, J., Duboule, D., Durston, A. J., Kmita, M., Nicolas, J. F., Palmeirim, I., Smith, J. C. and Wolpert, L. (2006). Head-tail patterning of the vertebrate embryo: one, two or many unresolved problems? *Int. J. Dev. Biol.* **50**, 3-15.

Tam, P. P. and Tan, S. S. (1992). The somitogenetic potential of cells in the primitive streak and the tail bud of the organogenesis-stage mouse embryo. *Development* **115**, 703-715.

Trainor, P. and Krumlauf, R. (2000). Plasticity in mouse neural crest cells reveals a new patterning role for cranial mesoderm. *Nat. Cell Biol.* **2**, 96-102.

Tucker, A. S. and Slack, J. M. (1995). Tail bud determination in the vertebrate embryo. *Curr. Biol.* **5**, 807-813.

Uehara, M. and Ueshima, T. (1988). Studies of neural tube development in the chicken embryo tail. *Anat. Embryol.* **179**, 149-155.

Yamaguchi, T. P., Bradley, A., McMahon, A. P. and Jones, S. (1999). A Wnt5a pathway underlies outgrowth of multiple structures in the vertebrate embryo. *Development* **126**, 1211-1223.

DEVELOPMENT